PHYSICAL REVIEW E **86**, 041705 (2012)

Critical behavior of a nonpolar smectogen from high-resolution birefringence measurements

Selen Erkan, Mehmetcan Çetinkaya, Sevtap Yildiz, and Haluk Özbek[*]
Department of Physics, Istanbul Technical University, 34469 Maslak, Istanbul, Turkey

(Received 28 June 2012; published 11 October 2012)

We report high-sensitivity and high-temperature resolution experimental data for the temperature dependence of the optical birefringence of a nonpolar monolayer smectogen 4-butyloxyphenyl-4′-decyloxybenzoate ($\overline{10}$.O.$\overline{4}$) liquid crystal by using a rotating-analyzer technique. The birefringence data cover nematic and smectic-A phases of the $\overline{10}$.O.$\overline{4}$ compound. The birefringence data are used to probe the temperature behavior of the nematic order parameter $S(T)$ in the vicinity of both the nematic-isotropic (N-I) and the nematic–smectic-A (N-SmA) transitions. For the N-I transition, from the data sufficiently far away from the smectic-A phase, the average value of the critical exponent β describing the limiting behavior of $S(T)$ is found to be 0.2507 ± 0.0010, which is in accordance with the so-called tricritical hypothesis, which predicts $\beta = 0.25$ and excludes higher theoretical values. The critical behavior of $S(T)$ at the N-I transition is discussed in detail by comparing our results with the latest reports in the literature and we conclude that by comparing with the previously reported results, the isotropic internal field assumption by the Vuks-Chandrasekhar-Madhusudana model is adequate to extract the critical behavior of $S(T)$ from the optical birefringence data. We observe that there is no discontinuous behavior in the optical birefringence, signaling the second-order nature of the N-SmA transition. The effect of the coupling between the nematic and smectic-A order parameters on the optical birefringence near the N-SmA transition is also discussed. In a temperature range of about 4 K above and below the N-SmA transition, the pretransitional evidence for the N-SmA coupling have been detected. From the analysis of the optical birefringence data above and below the N-SmA transition by means of various fitting expressions we test the validity of the scaling relation $\lambda = 1 - \alpha$ between the critical exponent λ describing the limiting behavior of the nematic order parameter and the specific heat capacity exponent α. We then show that the temperature derivative of the nematic order parameter $S(T)$ near T_{NA} exhibits the same power-law divergence as the specific heat capacity with an effective critical exponent of 0.2303 ± 0.0035.

DOI: 10.1103/PhysRevE.86.041705 PACS number(s): 64.70.M−, 78.15.+e, 42.70.Df, 61.30.−v

I. INTRODUCTION

Liquid crystals (LCs) constitute a state of matter that has properties between those of a crystalline solid and an isotropic liquid. Many liquid crystalline compounds exhibit one or more distinct mesophases between the crystalline solid and the isotropic liquid. These mesophases are classified on the basis of molecular order. Most common mesophases are orientationally ordered nematic (N) phases and the layered smectic (Sm) phases [1,2]. Without any long-range positional order, the nematic phase is characterized by long-range orientational order where the molecules tend to align along a preferred direction, the so-called director. In smectic phases, in addition to long-range orientational order, partial positional order is present as well. In the smectic-A (SmA) phase, a one-dimensional layering structure, normal to the layers parallel to the director, occurs.

A nematic liquid crystal, due to its orientational order, behaves like an optically uniaxial crystal and its physical properties exhibit anisotropy [1,3]. As pointed out by de Gennes [1], any anisotropic physical quantity can be a measure of orientational ordering in the nematic phase. Among these quantities, the optical birefringence is a crucial parameter with respect to practical applications of liquid crystals since in each type of nematic display an optimum birefringence value is required to obtain a maximum optical contrast [4,5]. In contrast, the birefringence is of great importance since it is directly proportional to the orientational order parameter of the N phase. Furthermore, it is worthwhile noting that the knowledge of the temperature dependence of the orientational order parameter is essential for testing any model of liquid crystalline behavior [6].

It is well known that interference methods [4] are often used to measure the optical birefringence. To date, the wedge method [7], the light transmission method for plane-parallel liquid crystal cells [8–10], and the conoscopic method [11] have been frequently used. Recently, a modulated polarization technique for birefringence measurements has been reported [12,13]. In addition it should be noted that birefringence measurements have concentrated almost solely on homologous series of 4-alkyl-4′-cyanobiphenyl (nCB) and 4-alkyloxy-4′-cyanobiphenyl (nOCB) [14] liquid crystalline compounds and their mixtures [7–9,11–13]. The nCB and nOCB compounds are known to have the strongly polar cyano end group. Thus the partial bilayer SmA phase, SmA_d, forms due to an antiparallel orientation between neighboring polar molecules such that the aromatic cores overlap [15]. Nevertheless, in the literature one can find numerous studies on the critical behavior of the orientational (nematic) order parameter $S(T)$ obtained from refractive index or birefringence measurements directly [16–21]. However, the above-mentioned studies on the critical behavior of the order parameter $S(T)$ have focused mostly on the nematic-isotropic (N-I) transition, except for the studies in Refs. [17,21]. In most studies [18–20] the analysis of the order parameter $S(T)$ has been performed via the Haller approximation [22], which is known to be inconsistent with the weakly first-order character of the N-I transition [23,24].

---

[*] Corresponding author: hozbek@itu.edu.tr

In fact, the critical exponent β of the order parameter $S(T)$ found by this approximation has values in between 0.14 and 0.2 [18–20] that do not match any of the predicted theoretical values. Recently, it has been shown [16,17] that the Haller approximation is not acceptable in the analysis of the order parameter $S(T)$ since it leads systematically to lower values for β, namely, $\beta \leqslant 0.20$, than those extracted from refractive index [16,17], dielectric constant anisotropy [25,26], and anisotropy in thermal conductivity data [27]. Another issue is that not only the temperature resolution but also resolutions in refractive index and birefringence measurements are insufficient to extract the limiting behavior of the exponent β discussed in the above studies since refractive index [18,19] and birefringence measurements [20] are based on the visual inspection by means of an Abbe refractometer and wedge method for the former and Newton's ring technique for the latter. Thus it should be emphasized that high-resolution (in both temperature and birefringence) measurements are essential in order to extract the critical behavior near the phase transition region.

The nematic–smectic-A (N-SmA) transition in liquid crystals has been studied extensively [23,24,28,29], but it still remains one of the most intriguing problems in the statistical mechanics of condensed matter. Although one can find several refractive index or optical birefringence studies covering the N and SmA phases in the literature [11,21,30], quite surprisingly, the number of high-resolution (in both temperature and birefringence) optical studies is quite limited especially in the vicinity of the N-SmA transition. Lim and Ho [31] measured the birefringence in polar liquid crystal 8OCB [14] in order to reveal the behavior of the nematic order parameter near the N-SmA transition. They did not observe any measurable discontinuity in the birefringence, signaling the second-order nature of the transition. They remarked that improvements beyond mean-field molecular and phenomenological theories are essential to clarify pretransitional temperature behavior, due to fluctuations, of the birefringence in the vicinity of the N-SmA transition. In addition, Gramsbergen and de Jeu [32] measured the birefringence of mixtures of two compounds, namely, $n = 7$ and 8, of the homologous series of nonpolar p,p'-dialkylazoxybenzenes (nAB) near the N-SmA transition. The tricritical N-SmA point was observed for a mole fraction near 0.5 of the 8AB liquid crystal in the mixture. At lower mole fractions of 8AB, for the second-order transitions, the critical exponent λ describing the limiting behavior of the nematic order parameter in the vicinity of the N-SmA transition was found to increase with decreasing 8AB concentration from the value of 0.51 for the tricritical mixture to 0.64 for the pure 7AB compound. They noted that the critical exponent values were in good agreement with the ones extracted from x-ray scattering experiments [33]. However, since calorimetric information was not available, it was not possible to test the theoretically expected [34] relation $\lambda = 1 - \alpha$, where α is the specific heat capacity exponent. Very recently, Kityk *et al.* reported high-resolution optical birefringence measurements of 8OCB [12] and 7CB–8CB [13] imbibed in silica channels and also compared their results to the bulk behavior. In these studies however, the critical behavior of birefringence near the phase transitions was not discussed. Furthermore, in Ref. [27] Marinelli and Mercuri reported high-resolution photopyroelectric (PPE) measurements of the anisotropy in the thermal conductivity in the nCB ($n = 5$–9) homologous series. They used the data to deduce the critical behavior of the nematic order parameter $S(T)$ close to the N-I and N-SmA transitions of 8CB and 9CB LC compounds in particular. They developed a simple model taking into account the contribution of fluctuations to the orientational order close to the N-SmA transition. Within the framework of the model, the authors used the critical exponent $1 - \alpha$ directly to quantify the limiting behavior of the nematic order parameter near the N-SmA transition [see Eqs. (8) and (9) in Ref. [27]]. Instead of testing the theoretically expected relation $\lambda = 1 - \alpha$, they used the values of specific heat capacity exponents directly given in the literature [23,28,29] to analyze their data. Another issue is that the scaling condition $S(T = 0\ \mathrm{K}) = 1$ [16,17] for the order parameter $S(T)$ is not fulfilled in the data analysis given in Ref. [27] since the PPE technique does not give the $S(T)$ value but only a quantity proportional to it because of the very complicated connection between thermal conductivity and microscopic processes of heat transport as argued by Marinelli and Mercuri [27].

The nonpolar 4-alkyloxyphenyl-4′-alkyloxybenzoate ($\overline{n}$.O.$\overline{m}$) liquid crystalline compounds [35], in contrast to nCB and nOCB compounds, do not exhibit antiparallel ordering and have a normal monolayer smectic A, namely, SmA_m, phase [36]. In contrast, the N-I and N-SmA transitions in $\overline{n}$.O.$\overline{m}$ compounds have not been investigated systematically. The $\overline{6}$.O.$\overline{8}$, $\overline{6}$.O.$\overline{10}$, and $\overline{6}$.O.$\overline{12}$ compounds and their mixtures have been investigated only by adiabatic scanning calorimetry [29,37,38]. Additionally, both the SmA-SmC transition in pure $\overline{10}$.O.$\overline{4}$ and the SmA-SmC^* (chiral SmC) transition in the binary mixtures of $\overline{10}$.O.$\overline{4}$ with methyl-choloropentanoyloxy heptyloxybiphenyl ($C7$) liquid crystals have been studied via x-ray measurements for the former [39] and ac calorimetry [40], NMR spectroscopy [41], and electroclinic tilt susceptibility measurements [42] for the latter. Yildiz and Nesrullajev investigated the effect of surface aging on thermotropic properties of $\overline{10}$.O.$\overline{4}$ by means of polythermic polarizing microscopy technique [43]. The mirage effect in particular was used to study SmA-SmC transitions in $\overline{10}$.O.$\overline{4}$-$\overline{8}$.O.$\overline{4}$ binary mixtures by Özbek *et al.* [44]. The effect of thin films on the orientational and optical properties of $\overline{10}$.O.$\overline{4}$ has also been studied by the mirage effect [45]. Results for the N-SmA transitions of the $\overline{10}$.O.$\overline{4}$ compound have been reported from studies based on refractive index measurements [17] and calorimetric methods [46]. Recently, Gupta *et al.* reported the temperature dependence of optical birefringence of $\overline{10}$.O.$\overline{6}$ liquid crystal in nematic, smectic-A, and smectic-C phases [47] by means of the Chatelain-wedge principle. Although the birefringence measurements cover nematic and smectic-A phases, the authors did not argue the critical behavior of the order parameter of the $\overline{10}$.O.$\overline{6}$ liquid crystal since the temperature resolution was insufficient. In contrast, in Ref. [17] Yildiz *et al.* measured the ordinary and extraordinary refractive indices of $\overline{10}$.O.$\overline{4}$ by means of an Abbe refractometer. As has been repeatedly stated, these types of measurements are based on visual inspection; thus the resolution in the birefringence is poor. Due to a lack of information about the critical behavior of the nematic order parameter, particularly in the vicinity of the N-SmA transition, recently we have focused on high-resolution optical birefringence measurements based on a rotating-analyzer method, which is a very accurate interference method [32,48,49]. It is well known that the optical birefringence is a direct measure of the nematic order parameter. Furthermore, it is also sensitive to the smectic order parameter, as will be discussed in more detail in the following section. The rotating-analyzer method has been known for a long time; quite surprisingly it has not been used for optical birefringence measurements. The method has a resolution as high as the one used by Kityk *et al.* [12,13].

The aim of the present work is to focus on the critical behavior of the nematic order parameter near both the N-I and the N-SmA transitions in $\overline{n}$.O.$\overline{m}$ compounds since large terminal dipoles are absent in these compounds contrary to nCB and nOCB liquid crystals. With this purpose in mind, we report high-resolution (in both the birefringence and temperature) optical birefringence data for a $\overline{10}$.O.$\overline{4}$ LC covering the nematic and the smectic-A phases. It is worthwhile noting that this high-resolution optical birefringence study investigates the temperature dependence of the optical birefringence of $\overline{n}$.O.$\overline{m}$ nonpolar monolayer smectogens. Here we discuss the critical behavior of the nematic order parameter at the N-I transition in detail by comparing our results with the latest reports in the literature. We also discuss the effect of the coupling between the nematic and smectic-A order parameters on the optical birefringence in the vicinity of the N-SmA transition. Moreover, by analyzing the temperature behavior of both optical birefringence Δn directly and also its temperature derivative near the N-SmA transition, we have tested the validity of the scaling relation $\lambda = 1 - \alpha$ between the critical exponent λ describing the limiting behavior of the nematic order parameter and the specific heat capacity exponent α in the vicinity of the transition, contrary to the analysis carried out by Marinelli and Mercuri in Ref. [27].

II. THEORETICAL BACKGROUND

A. Nematic-isotropic transition

In the nematic phase, for rodlike molecules, the simplest measure of the long-range orientational order of a liquid crystal is given by the scalar order parameter $S(T)$, introduced by Tsvetkov [50]:

$$S = \tfrac{1}{2}\langle 3\cos^2\theta - 1\rangle, \tag{1}$$

where θ describes the orientation of the molecular symmetry axis with respect to the director and it depends strongly on temperature T. The angular brackets denote an averaging over all molecules under consideration. As far as the optical measurements, refractive index, or optical birefringence are concerned, to determine the behavior of $S(T)$ one needs to develop a molecular model connecting the macroscopic property (i.e., optical birefringence) to the related molecular property, namely, the polarizability α. Two models have been extensively applied, namely, the isotropic model by Vuks, Chandrasekhar, and Madhusudana [51] and the anisotropic model by Neugebauer, Maier, and Saupe [52]. The Vuks-Chandrasekhar-Madhusudana (VCM) model assumes an isotropic internal field experienced by a molecule. The nematic order parameter $S(T)$, under the assumption of the VCM model, is given by

$$\frac{\Delta\alpha}{\langle\alpha\rangle}S(T) = \frac{n_e^2 - n_o^2}{\langle n^2\rangle - 1}, \tag{2}$$

where n_e and n_o are the extraordinary and ordinary refractive indices, respectively, and $\langle n^2\rangle = (n_e^2 + 2n_o^2)/3$. The molecular polarizability anisotropy is given by $\Delta\alpha = \alpha_l - \alpha_t$, where α_l and α_t are longitudinal (parallel) and transverse (perpendicular) polarizabilities relative to the long molecular axis, respectively. The mean polarizability, which is an intrinsic temperature-independent molecular property [19,21,47], is $\langle\alpha\rangle = (\alpha_l + 2\alpha_t)/3$. The optical anisotropy, or optical birefringence, depends on the wavelength and temperature and is defined as

$$\Delta n = n_e - n_o = n_\parallel - n_\perp, \tag{3}$$

where $n_\parallel$ and $n_\perp$ are the refractive indices parallel and perpendicular to the director, respectively. Noting that $n_e^2 - n_o^2 = 2\overline{n}(\Delta n)$, where $\overline{n} = (n_e + n_o)/2$, it is plausible to take that $\overline{n} \approx \overline{n}_I$ and $\langle n^2\rangle \approx \overline{n}^2 \approx n_I^2$, where n_I is the value of the refractive index in the isotropic phase just above the N-I transition temperature T_{NI}. With the help of these approximations, Eq. (2) can be written as

$$\frac{\Delta\alpha}{\langle\alpha\rangle}S(T) = \frac{2n_I\Delta n}{n_I^2 - 1}. \tag{4}$$

This approximation seems excellent due to partial cancellation of the changes resulting from small variations in $\overline{n}$ with temperature T [16,17].

Particularly noteworthy is the fact that the temperature dependence of the order parameter S in the nematic phase turns out to be quite complicated since there is no analytic solution to the quartic equation arising from the minimization condition of the Landau–de Gennes expansion [1,53]. However, the behavior of $S(T)$ in the nematic phase can still be well approximated by a four-parameter power-law expression, which is consistent with the mean-field theory for a critical as well as a tricritical point for a weakly first-order transition (nonzero cubic term) [23,25,37,53]. The temperature dependence of $S(T)$ can be written as

$$S(T) = S^{**} + A|\tau|^\beta, \tag{5}$$

where $\tau = (T - T^{**})/T^{**}$ is the reduced temperature relative to the effective second-order transition temperature T^{**} seen from below T_{NI}, i.e., the absolute limit of the superheating of the nematic phase, and is slightly larger than the observed transition temperature T_{NI}. At $T = 0$ K, the nematic order would become perfect; hence a plausible scaling condition for $S(T)$ is given by $S(0) = 1$, which implies $S^{**} + A = 1$. In order to quantify the birefringence measurements we used the following expression derived from Eqs. (4) and (5) together with the scaling condition given above:

$$\Delta n = \frac{n_I^2 - 1}{2n_I}\frac{\Delta\alpha}{\langle\alpha\rangle}[S^{**} + (1 - S^{**})|\tau|^\beta]. \tag{6}$$

This expression contains four fit parameters $\Delta\alpha/\langle\alpha\rangle$, S^{**}, T^{**}, and β. The n_I value is quoted from refractive index measurements [17]. Previous attempts to extract the critical behavior of the order parameter $S(T)$ have assumed a smaller number of free parameters for the fitting procedure. Haller's approximation [22] consists of determining $\Delta\alpha/\langle\alpha\rangle$ and β from an expression similar to Eq. (5) in which $S^{**} = 0$ and $T^{**} = T_{NI}$. Only points far from T_{NI} have been considered in the fitting procedure [18–20]. As argued previously, this approximation gives systematically lower values for β and is not consistent with the character of the N-I transition.

B. Nematic–smectic-*A* transition

In liquid crystalline compounds exhibiting the smectic-A phase as well as the nematic phase, it is reasonable to expect that the orientational ordering is augmented by the occurrence of the smectic layering and this augmentation will probably depend on the strength of the coupling between the nematic and smectic-A order parameters. For the coupling of the nematic order parameter S with the smectic-A order parameter Ψ, de Gennes postulated [54] the relationship $S - S_0 = C\chi\langle|\Psi|\rangle^2$ in the mean-field approach. Here S_0 is the value of S in the absence of smectic ordering, C is a coupling constant, and χ is a response function. By including the effect of short-range smectic ordering and the fluctuations of the order parameters, this form has to be modified [31] into $S - S_0 \sim \langle|\Psi|^2\rangle$. Based on a rather general consequence of the Landau–de Gennes free energy [33,34,54], one can derive the following expression:

$$\langle|\Psi|^2\rangle = A + B_\pm|t|^\lambda, \tag{7}$$

where $t = (T - T_{NA})/T_{NA}$, with T_{NA} the N-SmA transition temperature, and $\lambda = 1 - \alpha$, with α the specific heat capacity exponent. The plus-minus sign refers to above and below T_{NA}, respectively. As mentioned previously, there is a quite general argument predicting the relation $\lambda = 1 - \alpha$ for the Landau–de Gennes free energy. Simply, the argument starts with the free energy of the form $U = \int d^3r[at|\Psi|^2 + \delta U(\Psi)]$ and then calculates the partition function $Z = \int d\Psi \exp(-U/k_BT)$. Differentiation with respect to temperature yields the excess entropy $\Delta S^* \sim \langle|\Psi|^2\rangle$. Then ΔS^* can be calculated by taking the integral of the singular part of the specific heat capacity $C_P \sim t^{-\alpha}$; thus $\Delta S^* \sim \langle|\Psi|^2\rangle \sim t^{1-\alpha}$ and finally one obtains $\lambda = 1 - \alpha$. As discussed in Sec. II A, the relation between the optical birefringence Δn and the order parameter S is rather complex due to the internal field problem, but as a first approximation it is reasonable to assume that they are proportional. Thus, with the help of the relation $S - S_0 \sim \langle|\Psi|^2\rangle$, it is possible to determine the critical exponent λ in Eq. (7) from high-resolution Δn vs T data in the vicinity of the N-SmA transition and to justify the relation $\lambda = 1 - \alpha$ by comparing the specific heat capacity exponent α in the literature when available.

III. EXPERIMENT

The nonpolar smectogen liquid crystal 4-butyloxyphenyl-4′-decyloxybenzoate ($\overline{10}$.O.$\overline{4}$) $C_{10}H_{21}O$-Ph-COO-Ph-OC_4H_9, where Ph refers to a benzene ring, was synthesized and purified by Dabrowski in the Institute of Chemistry, Military University of Technology, Warsaw, Poland. By chromatography, the purity was stated to be better than 99.8% and the compound was used as received.

In this work we employed high-resolution (in both temperature and birefringence) optical birefringence measurements to reveal the critical behavior of the $\overline{10}$.O.$\overline{4}$ compound. We performed the optical measurements via the rotating-analyzer method [32,48,49]. In this method, light from a He-Ne laser (JDS Uniphase) at a wavelength of $\lambda = 633$ nm, passes successively through a polarizer (Thorlabs Inc.), the sample, a quarter-wave plate (Thorlabs Inc.), and a rotating polaroid with angular frequency ω before reaching a photodiode (Thorlabs Inc.). The polarizer and the quarter-wave plate are both oriented at an angle of 45° to the optical axis of the planar-oriented sample. Note that the phase of the ac signal at the photodiode is directly proportional to the birefringence of the sample. A reference beam from another laser module passes through the rotating polaroid onto another photodiode. Thus two signals are modulated with an angular frequency of 2ω. (For more details, see Refs. [32,49].) Note that the light transmitted by the sample is elliptically polarized with an ellipticity expressed as a phase retardation of δ, given by $\delta = (2\pi d/\lambda)\Delta n$. Here d refers to the sample thickness. Passing through the quarter-wave plate, the elliptically polarized light is converted to the plane polarized light rotated through half the ellipticity angle. This angle is very accurately determined via the rotating polaroid and thus the phase angle of the rotated light is measured relative to the reference beam. The block diagram of the setup is given in Fig. 1. The phase measurements were made with an accuracy of 10^{-4} rad, with the help of lock-in detection (Stanford Research, SR830). In our setup the sensitivity in Δn of 10^{-6} was obtained for a 20-μm-thick sample. The temperature was measured and controlled by an resistance temperature detector sensor (Omega Eng. Corp.) and a LakeShore Model 331 temperature controller with a resolution of 0.001 K, respectively. It is worth recalling that the rotating analyzer setup is fully computer-controlled via LABVIEW (National Instruments) software. The resulting arbitrariness in Δn was removed by using the samples with various thicknesses, namely, 18 and 20 μm.

It is well known that for accurate measurements of S and other relevant optical parameters the LC samples need to be well aligned. The $\overline{10}$.O.$\overline{4}$ sample was introduced by capillary filling in the isotropic phase into a LC cell, which was purchased from Instec Inc., with a thickness of 20 μm, and then prepared to produce planar orientation of LC molecules. After the filling process the LC cell was sealed with an epoxy cement. The exact thickness of the empty cell was checked

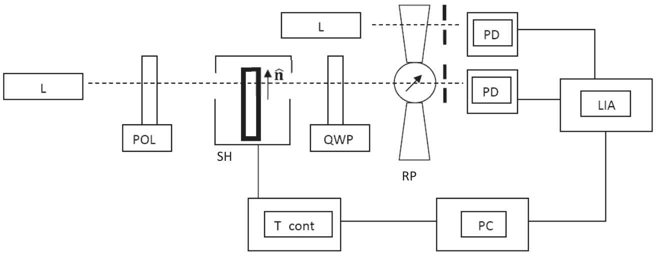

FIG. 1. Schematic diagram of the high-resolution rotating analyzer setup: L, laser; POL, polarizer; SH, sample holder; QWP, quarter wave plate; RP, rotating polaroid; PD, photodiode; LIA, lock-in amplifier; T cont, temperature controller; PC, computer. The arrow shows the director $\hat{n}$.

both interferometrically (Jasco V-530 UV-visible spectrophotometer) and via scanning electron microscopy. Additionaly, the microscopy observations were carried out with an Olympus BHSP polarizing microscope equipped with a homemade hot stage and with a EMKO ESM 9320 digital PID temperature controller in order to identify the structure of the mesophases, to confirm the phase transition temperatures and to check the planar alignment of the LC cells as well. The optical birefringence measurements were performed for several cooling and heating runs and reproducible results were obtained.

IV. RESULTS and DISCUSSION

A. Nematic-isotropic transition

In Fig. 2 the optical birefringence Δn vs temperature T data of $\overline{10}$.O.$\overline{4}$ upon cooling (with the average scanning rate of 1.8 mK/min) from isotropic liquid to the SmA phase is displayed. In the isotropic phase the birefringence is zero and increases with decreasing temperature as expected. We considered the N-I transition temperature T_{NI} to be the lowest temperature corresponding to the zero birefringence in the isotropic phase. Thus the observed transition temperature was $T_{NI} = 359.54$ K. Thus it can be concluded that any pretransitional effects are absent in the isotropic phase. Moreover, the overall shape of the Δn vs T behavior is in good agreement with similar studies for various rodlike LCs [12,13]. As seen in Fig. 2, an enhancement in Δn takes place upon lowering the temperature towards the SmA phase. The Δn is enhanced as the smecticlike short-range order builds up, reflecting the enhancement in the nematic (orientational) order parameter. It should be pointed out that due to the considerably higher resolution, our Δn measurements can be used to describe more precisely the nature of the N-SmA transition, as will be discussed below. Note that the N-I and N-SmA transition temperatures were also confirmed by texture changes in the polarizing microscope.

In order to reveal the critical behavior of the nematic order parameter $S(T)$ near the N-I transition the experimental Δn vs T data have been fitted to Eq. (6). For the fitting procedure, we have used a nonlinear multiparameter fitting program using a subroutine of MATLAB, based on the conjugated gradient method, which has been used successfully up to now [16,17,45,46]. The quality of the fits has been evaluated via the reduced error function χ_ν^2, which is defined as [55]

$$\chi_\nu^2 = \frac{\frac{1}{\nu}\sum_i (y_i - f_i)^2}{\sigma^2}, \tag{8}$$

where $\nu = N - p$ is the degrees of freedom, with N the number of data points and p the number of fit parameters. In Eq. (8) y_i is the ith measurement value and f_i is the corresponding fit value. Here σ^2 refers to the variance of the data. Following this definition, a good fit yields $\chi_\nu^2 \approx 1$–1.5. The results of the fits are summarized in Table I. The stability of the fit results was tested by a double range shrinking technique in which the points situated at both ends of the data set were gradually discarded and the data refitted. At the high-temperature side some data points had to be eliminated due to the fact that they were very close to the transition temperature T_{NI} and probably in the coexistence region. Additionally, since $\overline{10}$.O.$\overline{4}$ LC exhibits the N-SmA transition at $T_{NA} = 349.37$ K, the influence of the pretransitional behavior of the SmA phase was detected in the nematic phase. We observed that this pretransitional smectic behavior continues to 4.1 K above the N-SmA transition temperature. Thus the range shrinking procedure at the low-temperature side of the nematic phase indicated that only the 5.9-K data range was available for the fitting procedure in the N phase. Due to the high resolution, we had enough data points (2950 points typically) to get reasonably fit results. Based on the refractive index data, Chirtoc *et al.* reported [16] a similar pretransitional behavior of the SmA phase for polar LC 8CB continuing up to 4 above T_{NA}.

As seen from Table I, the average value of the temperature difference $T^{**} - T_{NI}$ is found to be 0.24 ± 0.03 K. Note that the value of 0.21 ± 0.04 K on average for $T^{**} - T_{NI}$ was reported for the nCB homologous series based on refractive index data by Chirtoc *et al.* [16]. In contrast, we previously obtained a value of 0.16 ± 0.04 K for this difference by using refractive index data [17]. Since the resolution of the refractive index measurements is not as good as that obtained by the method presented here the result $T^{**} - T_{NI} = 0.24 \pm 0.03$ K seems more reliable. In the literature one can find some reported results for $T^{**} - T_{NI}$ based on various experimental techniques to compare with our results. Cusmin *et al.* reported that $T^{**} - T_{NI} \approx 0.073$ K for the 9OCB compound based on the specific heat capacity, dielectric constant, and molar volume measurements [56]. Rzoska *et al.* found -0.2 and -0.09 for 6OCB and 7OCB LCs, respectively, by dielectric constant measurements [57] having no physical significance. Moreover, Zywocinski found $T^{**} - T_{NI} \approx 0.11$ for 8CB following molar volume data [58]. The $T^{**} - T_{NI}$ values from specific heat capacity measurements are known to be one order of magnitude smaller than the values obtained from several other quantities [38]. Thus the main conclusion drawn here is that the optical measurements seem to be more appropriate to get reliable values for the spinodal temperature T^{**}. Additionally, we have found that $\Delta\alpha/\langle\alpha\rangle = 0.5314 \pm 0.0002$ on average using the refractive index value $n_I = 1.5654$ in the isotropic phase just above the N-I transition temperature

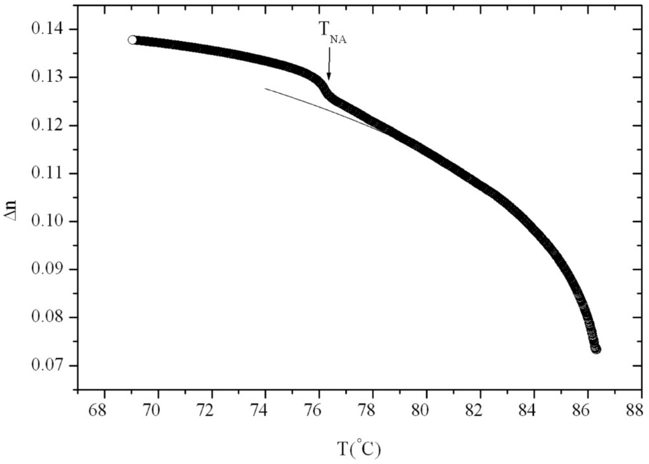

FIG. 2. Measured optical birefringence Δn vs temperature T of the $\overline{10}$.O.$\overline{4}$ compound. The arrow marks the N-SmA transition temperature. The solid line is the fit to Eq. (6) extrapolated to the SmA phase.

TABLE I. Parameter values obtained from the fitting of $\Delta n(T)$ data with Eq. (6) in the N-phase $\overline{10}$.O.$\overline{4}$. Quantities in square brackets were held fixed. The molar mass of $\overline{10}$.O.$\overline{4}$ is 426.602 g/mol.

$\Delta\alpha/\langle\alpha\rangle$	S^{**}	T^{**} (K)	β	χ_ν^2
0.5316 ± 0.0002	0.1523 ± 0.010	359.78 ± 0.11	0.251 ± 0.003	1.09
0.5312 ± 0.0018	0.1515 ± 0.010	359.77 ± 0.06	[0.25]	1.09
0.2148 ± 0.082	[0]	[359.54]	0.155 ± 0.016	3.4

T_{NI} of the $\overline{10}$.O.$\overline{4}$ LC [17]. Notice that in the present work we have used a He-Ne laser of wavelength 633 nm. It is worthwhile noting that the obtained value of $\Delta\alpha/\langle\alpha\rangle$ from refractive index measurements by means of an Abbe-type refractometer with a light source of wavelength 589.3 nm is lower by 6.7% than the one found in the present work [17]. In Ref. [16] Chirtoc *et al.* argued that the parameter $\Delta\alpha/\langle\alpha\rangle$ is wavelength dependent whereas the others are not. The authors also observed that the values of $\Delta\alpha/\langle\alpha\rangle$ determined using a 589.3-nm-wavelength light source are lower than those determined using a 633-nm-wavelength laser source.

Depicted in Figs. 3(a) and 3(b) are the profiles of the χ_ν^2 error function vs the fit parameters S^{**}, T^{**}, and β corresponding to the fits of the Δn vs T data. They were obtained from stepwise variation of the fit parameters S^{**}, T^{**}, and β, namely, in steps of 0.01, respectively. It should be noted that the minima of the corresponding profiles are in excellent agreement with those obtained from the four-parameter fitting procedure. The average value of the critical exponent β deduced from the χ_ν^2 error function profile was found to be $\langle\beta\rangle = 0.2507 \pm 0.0010$, with a smaller standard deviation than those of the individual fits. From the exponent value given in Table I and the high-resolution measurements of the optical birefringence in the present work, it can be concluded that within the limit of experimental uncertainties, the critical exponent of the nematic order parameter is in agreement with the value given by the tricritical hypothesis (TCH) with $\beta = 0.25$ and excludes higher theoretical values. Notice that in our previous study based on refractive index measurements [17], the critical exponent β for the N-I transition was found to be 0.246. In the present work, due to the high sensitivity of our method, the exponent value is more reliable. It is worth noting that a similar tricritical value for the critical exponent β near the N-I transition has been obtained for the 8CB LC, which exihibits the Sm*A* phase apart from the N phase by refractive index measurements [16]. Hence one can conclude that the tricitical behavior in the vicinity of the N-I transition is valid for both LC compounds exhibiting the partial bilayer SmA phase and the monolayer smectic *A* phase, i.e., for LCs with or without a terminal dipole, respectively. Cusmin *et al.* have reported that in the vicinity of the N-I transition, the critical exponents $\alpha \approx 0.5$ and $\beta \approx 0.25$ based on the specific heat capacity, static dielectric constant, and molar volume measurements on 9OCB [56]; additionally Rzoska *et al.* extracted the critical behavior of the static dielectric constant near the N-I transition and reported that $\alpha \approx 0.5$ for 6OCB and 7OCB [57]. Notice that although the reported values of the spinodal temperatures are conflicting in those studies, the exponent values extracted from various physical quantities are in good agreement with the TCH. The tricritical hypothesis was proposed by Keyes [59] and Anisimov *et al.* [60,61]. According to the conjectures by Keyes, two competing nematic order parameters, namely, the uniaxial and biaxial order parameters, are expected to exhibit diverging fluctuations near the N-I transition even though the biaxial order parameter is zero in the nematic phase. Anisimov *et al.*, based on high-resolution specific heat capacity measurements, argued that the behavior of the N-I transition looks like that near a tricritical point because of the smallness of the third- and fourth-order term coefficients in the Landau–de Gennes expansion [1,61].

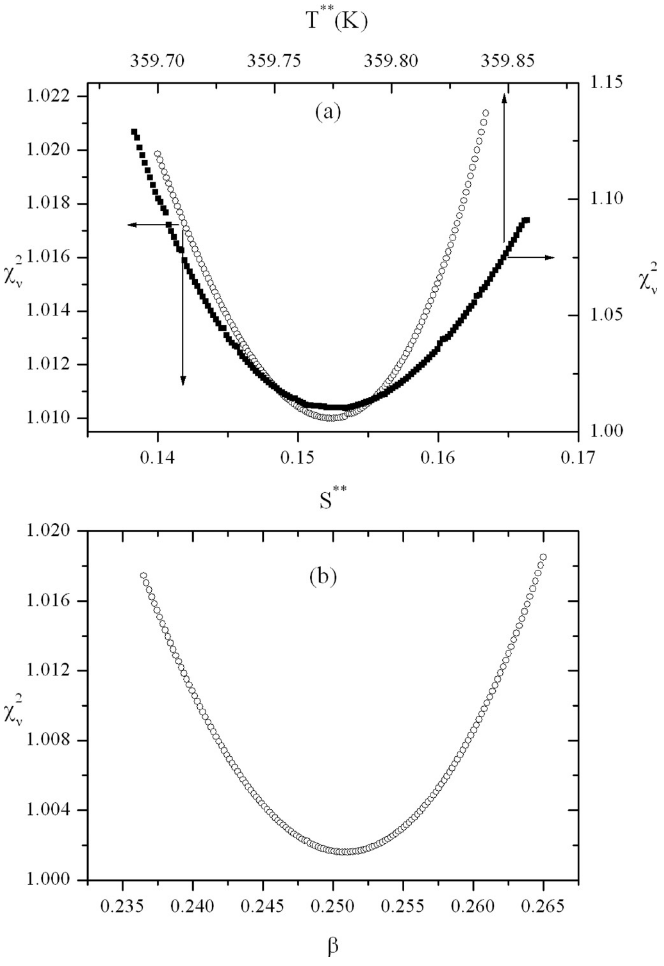

FIG. 3. Profiles of the error function χ_ν^2 obtained from stepwise variation of the fit parameters (a) S^{**} and T^{**} and (b) β.

Simoes and Simeao [62] studied the profile of the nematic order parameter derived from rescaled experimental data points by magnetic susceptibility anisotropy and dielectric anisotropy measurements. All investigated compounds present the N-I and the nematic-crystalline phase transitions, without any other liquid crystalline phase. They rescaled the data by defining the nematic temperature $t = (T - T_{NC})/(T_{NI} - T_{NC})$, where T_{NC} is the nematic-crystalline transition. Henceforth they showed that all experimental data coalesce along a common line that extends from the N-I transition region to the nematic-crystalline transition region. In order to quantify the data they used a similar expression given in Eq. (6) [see Eq. (2) in Ref. [62]]. They have found $\beta = 0.21 \pm 0.02$, which is quite close to the TCH value. Thereafter, Simoes *et al.* [63], by using experimental refractive index and thermal conductivity anisotropy data, investigated the behavior of the nematic order parameter in the entire nematic range for the LC samples exhibiting only an isotropic liquid, nematic, and crystalline phase sequence. They improved a recursive process that makes an independent and local calculation of the order parameter exponent β in the entire range of the N phase by using an equation similar to Eq. (6). They concluded that along the entire N range $\beta = 0.25$ which is the value given by the TCH.

However, it should be pointed out that the data used by Simoes *et al.* in Refs. [62,63] belong to LC compounds having only a nematic phase without any other liquid crystalline phase. In contrast, LCs compounds such as 8CB and $\overline{10}$.O.$\overline{4}$ exhibit pretransitional smectic behavior that continues up to 4 K above the N-SmA transition. It will be intriguing to investigate whether similar homogenous global behavior of the nematic order parameter $S(T)$ would be seen for LC compounds exhibiting pretransitional smectic behavior and whether there would be a universal pretransitional temperature range above T_{NA}. It is worth recalling that in order to decipher these behaviors various high-resolution experimental data, e.g., optical birefringence, dielectric anisotropy, and thermal conductivity anisotropy, are needed. We think that at least the present work is the beginning of high-resolution optical measurements to decipher the puzzle. A theory of the pretransitional smectic behavior above T_{NA} deserves systematic investigation both theoretically and experimentally.

Apart from the χ_ν^2 error function profiles vs the parameters S^{**} and β given in Fig. 3, Fig. 4 displays the correlation between the parameters S^{**} and β along the degenerate river on the χ_ν^2 surface as well. It could be clearly seen that the trajectory of the fitting procedure follows a curved path signaling the presence of an absolute maximum $S^{**}_{\max} = 0.165$. From the profiles in Fig. 3, one can realize why the Haller approximation ($S^{**} = 0$) gives deficient values for the exponent β. In Table I, to gain insight, we also included the fit results obtained via the Haller approximation, which gives lower values for β with large χ_ν^2 values. In Ref. [62] Simoes and Simeao observed that when the Haller approximation is used to fit all data $\beta = 0.159 \pm 0.003$ is found as well. As discussed in Sec. I, the studies given in Refs. [18–20,30] found values for β between 0.14 and 0.2. Although Kumari *et al.* [19], Pisipati and co workers [20] used the spinodal temperature T^{**} in the Haller expression instead of the N-I transition temperature T_{NI}, they reported that the T^{**} values are about 0.1–4 K higher than T_{NI}, which has no physical significance. Additionally Prasad and co-workers [18,30] asserted that the exponent β in the Haller expression depends on the molecular structure and its value is close to 0.2. Together with references given previously for the nCB homologous series, the present work shows that the value of the β exponent for the N-I transition is consistent with the TCH value and excludes the above conclusion. Our high-resolution optical birefringence measurements show that the N-I transition may not be a mean-field transition as argued by Maier and Saupe [1–3]. In order to highlight this point, in Fig. 5 we plot the nematic order parameter S of the $\overline{10}$.O.$\overline{4}$ LC as a function of temperature by using the present birefringence data and the fit results tabulated in Table I together with traditional theoretical models, namely, the Haller expression, the Maier-Saupe model [64], and the Picken model [65]. It is well known that the Maier-Saupe order parameter can be expressed approximately by the equation

$$S \cong \left(1 - \frac{yT}{T_{NI}}\right)^{z}, \tag{9}$$

where $y \cong 0.98$ and $z \cong 0.22$ for a series of experimental data [66]. Most materials gave $y = 0.98$–0.99 and $z = 0.14$–0.18. The semiempirical equation improved by Picken *et al.* [65],

$$S = 0.1 + 0.9\left(1 - 0.99\frac{T}{T_{NI}}\right)^{0.25}, \tag{10}$$

was found to describe S well for some homologous series at least. As seen in Fig. 5(a), the fit expression that we used to quantify our data [Eq. (6)] provides the best description of the nematic order parameter in comparison to traditional theoretical models excluding their validity near the N-I transition.

In Refs. [12,13] Kityk *et al.* used a modulated polarization technique for birefringence measurements of some LCs. In those studies they argued that it is sufficient to determine experimentally accessible Δn in order to obtain the molecular arrangement in a LC compound. They asserted that the temperature dependence of the bare refractive indices originates from changes in the anisotropic molecular polarizabilities of the single molecules. Then, in order to separate out these effects they used the quantity $\Delta n^* \propto \Delta n(T)[n_e(T) + n_o(T)]/2$ and called Δn^* an effective birefringence. Thus they argued that Δn^* is solely proportional to $S(T)$. However, it should be

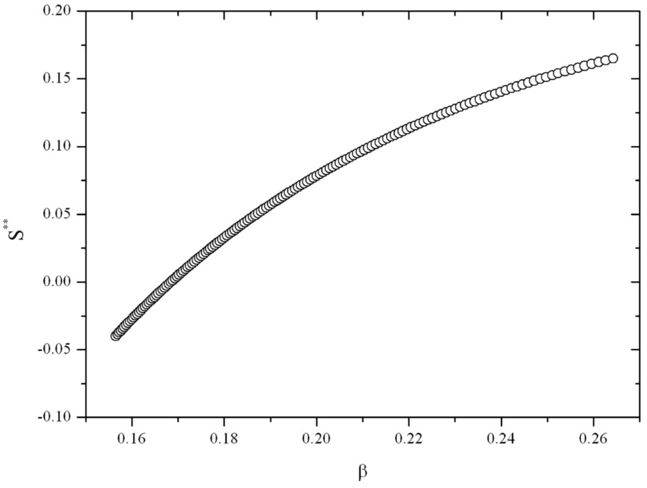

FIG. 4. Correlation of the four-parameter fit results in the (β, S^{**}) plane around the optimal values.

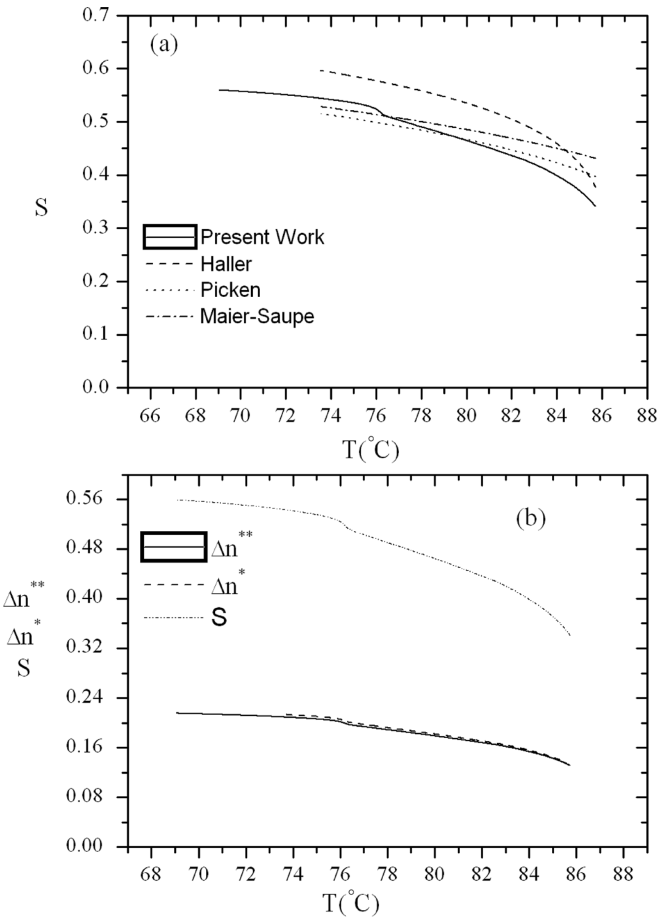

FIG. 5. (a) Nematic order parameter S vs temperature T determined from Eq. (4) together with the values in Table I. Dashed curves represent traditional theoretical models for the nematic order parameter S: the Haller approximation [Eq. (5) with S^{**} and $T^{**} = T_{NI}$], the Maier-Saupe model [Eq. (9)], and the semiempirical Picken equation [Eq. (10)]. (b) Effective birefringences (see the text) Δn^* vs T and Δn^{**} vs T and the nematic order parameter S vs T determined in the present work.

noted that in order to determine the temperature behavior of the effective birefringence one needs either the refractive indices n_e and n_o as functions of temperature T or to consult the literature data. In Fig. 5(b) we plot Δn^* vs T for $\overline{10}$.O.$\overline{4}$ generated from the present $\Delta n(T)$ data and the refractive index data given in Ref. [17]. As shown in Fig. 5(b), the nematic order parameter $S(T)$ of the $\overline{10}$.O.$\overline{4}$ LC obtained from the present work is higher than the effective birefringence $\Delta n^*(T)$ behavior. Hence it is unreliable to resort to the $\Delta n^*(T)$ data to represent the behavior of the order parameter $S(T)$. In contrast, in Sec. II A, while deriving Eq. (4), we have taken $\bar{n} = (n_e + n_o)/2 \approx n_I$. Thus it is reasonable to expect that the quantity $\Delta n^{**} \propto \Delta n(T) n_I$ should overlap with $\Delta n^*(T)$ [see Fig. 5(b)]. We can conclude that although the quantities $\Delta n^*$and Δn^{**} are deficient to represent the temperature behavior of $S(T)$, the approximation we have used to derive Eq. (4) is plausible. The last point to be emphasized here is that the isotropic internal field assumption by the VCM model and the approximation used while deriving Eq. (4) are adequate to extract the critical behavior of the order parameter $S(T)$ from the optical birefringence data.

B. Nematic–smectic-*A* transition

As stated previously, the study of the critical behavior at the N-SmA transition is an active area of research [23,24]. Most theoretical studies predict that this transition should belong to the three-dimensional (3D) XY universality class [1]. However, the experimental results to date have not established a clear case of 3D XY universality [23,24,28,29]. Owing to the coupling between the nematic and smectic-A order parameters, strongly influenced by the width of the nematic range, a crossover behavior from the second-order transition up to a tricritical point (TCP), beyond which the N-SmA transition is of first order, has been observed [23,24,28,29,36,56]. For a wide nematic range (weak coupling) the N-SmA transition is of second order. When the nematic range is narrow (strong coupling) the transition is of first order [28,29]. The McMillan ratio $R_M = T_{NA}/T_{NI}$ accounts for the coupling. Although the ratio R_M determines the width of the nematic range, its value is not universal for different systems. Additionally, the ratio R_M has been empirically used to locate the N-SmA TCP. Tricritical points have been characterized by the ratio of 0.942 to 0.995 [36,56], and systems with smaller ratios usually exhibit second-order N-SmA transitions.

In this section we focus on the coupling between the nematic and smectic-A order parameters near the N-SmA transition based on the optical birefringence data. It is worthwhile pointing out that the coupling, if it exists, manifests itself by an enhancement in the nematic order parameter S, thus in the Δn vs T data. In the nematic and smectic-A phases Δn and S are proportional to each other through quantities such as density and the mean refractive index, which are known to be insensitive to temperature [5,64]. Thus our high-resolution Δn vs T data perfectly reflect the effect on the order parameter S by the buildup of smectic-A ordering near the N-SmA transition. As one can infer from the extended plot in Fig. 6 and from the fact that no thermal hysteresis was observed within the

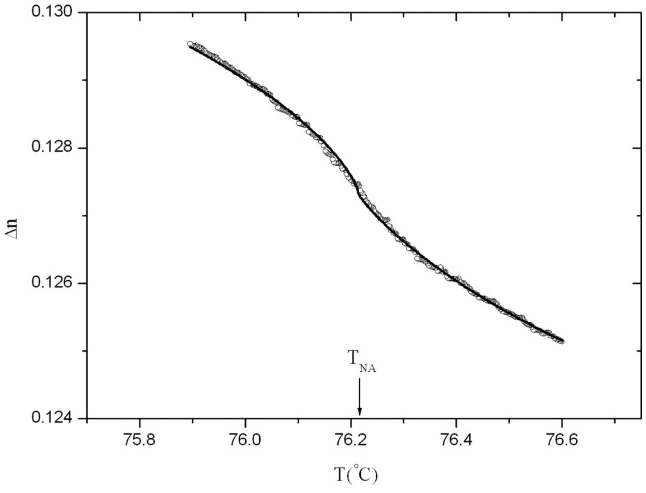

FIG. 6. Expanded plot of Δn vs temperature T in the vicinity of the N-SmA transition. The solid line is the fit to Eq. (13).

experimental resolution, the N-SmA transition of $\overline{10}$.O.$\overline{4}$ LC appears continuous.

In Fig. 2 it could be seen that there is an increment in the order parameter S induced by the occurrence of smectic layering above and below $T_{NA} \approx 349.37$ K. It is quite reasonable to infer that there should be an anomalous increase in the quantity $-d(\Delta n)/dT$ both above and below T_{NA} by inspecting the temperature behavior of the residuals $\Delta n_{\mathrm{exp}} - \Delta n_{\mathrm{fit}}$, with n_{fit} from the fitting in the nematic range of $\overline{10}$.O.$\overline{4}$ above $T_{NA} + 4.1$ K when the residuals are extrapolated down to a lower-temperature region. Kityk and Huber [12] have used the quantity $d(\Delta n)/dT$ to locate the phase transition temperatures. It should be noted here that both transition temperatures T_{NI} and T_{NA} of the $\overline{10}$.O.$\overline{4}$ LC extracted from the extrema of the $d(\Delta n)/dT$ vs T data are consistent with the ones obtained by polarizing microscopy and the supplier. Kityk and Huber [12] also argued that $d(\Delta n)/dT$ was related to the heat capacity anomaly based on the argument given in Sec. II B. In the present work, contrary to the approach by Kityk *et al.*, we have discussed whether the limiting behavior seen in the $d(\Delta n)/dT$ vs T data near T_{NA} is related to the specific heat capacity exponent α. Although it is possible to try numerical differentiation of the $\Delta n(T)$ data, the $-d(\Delta n)/dT$ calculated successively from the pairs of neighboring data points are too scattered, especially when the points are measured at rather small temperature steps, namely, 2–5 mK. Instead, it is admissible to introduce a new quotient such that

$$Q(T) = -\frac{\Delta n(T) - \Delta n(T_{NA})}{T - T_{NA}}. \tag{11}$$

One can easily show that if the $-d(\Delta n)/dT$ vs T data follows a power-law behavior with the critical exponent z, then the limiting behavior of the quotient $Q(T)$ follows a power law with the same critical exponent and the background term but different critical amplitude. A point that should be emphasized here is that the quotient $Q(T)$ is similar to the quantity $C(T) = [H(T) - H_c]/(T - T_c)$, with $H(T)$ the enthalpy obtained as a function of temperature T by adiabatic scanning calorimetry [23,67]. Likewise, the quantity $C(T)$, which is in fact the slope of the chord connecting $H(T)$ at T with H_c at T_c, has a power-law behavior with the same critical exponent α as the specific heat capacity $C_p = dH/dT$ [23,29,67]. This fact has frequently been exploited in the analysis of the enthalpy data [23,46,67,68]. Previously, another quotient $Q(T) = [V(T) - V_c]/(T - T_c)$, with $V(T)$ the molar volume obtained as a function of temperature T by a dilatometer [69], was used to analyze the molar volume data near T_{NA} for various liquid crystals. It should be underlined here that since the quotient $Q(T)$ has a regular background contribution that may result from the temperature dependence of Δn_{fit}, it is possible to eliminate this effect by defining the so-called the background quotient $Q_b(T) = -[\Delta n_{\mathrm{fit}}(T) - \Delta n_{\mathrm{fit}}(T_{NA})]/(T - T_{NA})$. In this manner the anomaly in the quotient $\Delta Q(T) = Q(T) - Q_b(T)$ can be observed more clearly as presented in Fig. 7 for the $\overline{10}$.O.$\overline{4}$ LC. Note that $\Delta Q(T)$ exhibits critical behavior near the N-SmA transition. As discussed previously in Sec. II B, the critical exponent z describing the behavior of the ΔQ vs T data near T_{NA} should be the same as that of the specific heat capacity and the volume thermal expansion coefficient, namely, α. Hence one can expect $z = \alpha = 1 - \lambda$. At this stage we would like to stress that the relationship between the critical exponents λ and α (see Sec. II B) can be deduced via the Lorenz-Lorentz relation between the refractive index and the density. When going from the nematic phase to the smectic-A phase, the increase in $\Delta n(T)$ and $S(T)$ is accompanied by an increase in the density [69,70]. That is, the increase in the nematic order parameter $S(T)$ is associated with a better packing of the molecules, due to induced smectic layering, and an associated density effect. Thus, on the basis of the generalized Pippard relations, the temperature behavior of the density and the volume thermal expansion coefficient have the same power-law divergence near a second-order phase transition as that of the specific heat capacity [71].

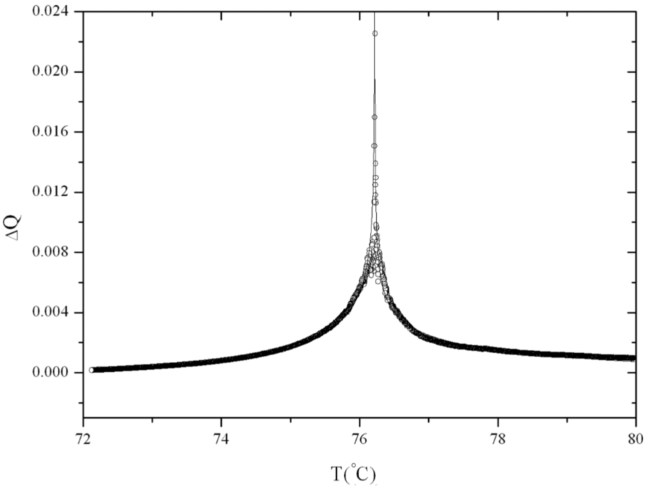

FIG. 7. Temperature behavior of the quotient $\Delta Q(T)$ in the vicinity of the N-SmA transition. The solid line is the fit to Eq. (12).

As an attempt to quantify the critical behavior of $\Delta Q(T)$ associated with the N-SmA transition the following fitting equation has been applied:

$$\Delta Q(T) = A_{\pm}|t|^{-z} + B, \tag{12}$$

with the critical amplitudes A_+ and A_- above and below T_{NA} and a background term B as well. Here $t = (T - T_{NA})/T_{NA}$ is the reduced temperature. Note that while fitting the ΔQ vs T data to Eq. (12) we have imposed the equality of the critical exponents below and above T_{NA} and fixed T_{NA} at 349.37 K. In Fig. 8 we present the χ_ν^2 error function profile of simultaneous fits of $\Delta Q(T)$ above and below T_{NA} as a function of the critical exponent z from the fitting procedure with three free parameters A_+, A_-, and B. As seen in Fig. 8, the minimum of the profile is in good agreement with the value determined from the four-parameter simultaneous fits. The minimum is found to be $z = 0.2301 \pm 0.0010$. Also note that the value of z from the four-parameter fitting is 0.2301 ± 0.0020. Previously, we performed adiabatic scanning calorimetry (ASC) measurements on the $\overline{10}$.O.$\overline{4}$ LC compound [46]. It is well known that ASC yields a temperature dependence of both the heat capacity and enthalpy. It can easily distinguish between the first- and second-order transitions and reveals subtle features of heat capacity [23,29,67]. Based on ASC data, we concluded that the N-SmA transition of $\overline{10}$.O.$\overline{4}$ is of

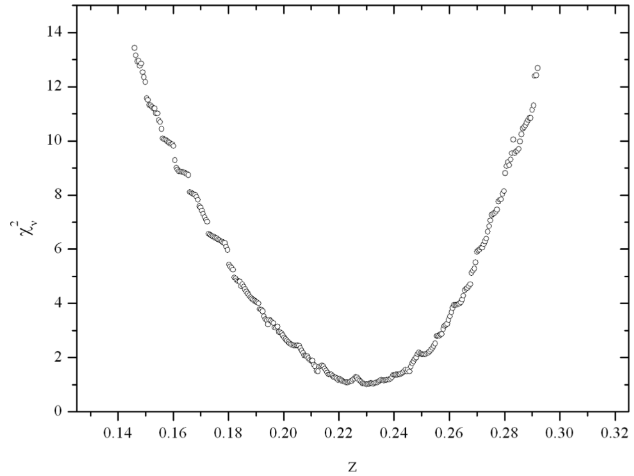

FIG. 8. The χ_ν^2 error function profile for fits of the $\Delta Q(T)$ data obtained from stepwise variation of the critical exponent z. The fitting function is given by Eq. (12).

second order within the experimental resolution and the value of the effective specific heat capacity critical exponent was found to be $\alpha = 0.23 \pm 0.01$ [46]. Note that there is excellent agreement between the z value extracted from optical $\Delta Q(T)$ data and the α value from calorimetric data. Thus it should be stressed that the temperature derivative of the nematic order parameter $S(T)$ curve below and above T_{NA} has the same power-law divergence as the specific heat capacity.

In order to get deeper insight into the critical behavior at the N-SmA transition of $\overline{10}$.O.$\overline{4}$ from our birefringence data and also to check the theoretically expected relation $\lambda = 1 - \alpha$ we have fitted our $\Delta n(T)$ data to the following expression, which is reminiscent of the fitting expression used to analyze the molar volume data in the literature [69,70]:

$$\Delta n(T) = \begin{cases} A'_+|t|^{1-z}(1 + D'_+|t|^{0.5}) + B'_+|t| + C'_+, & T > T_{NA} \\ A'_-|t|^{1-z'}(1 + D'_-|t|^{0.5}) + B'_-|t| + C'_-, & T < T_{NA}, \end{cases} \tag{13}$$

where $t = (T - T_{NA})/T_{NA}$. The fitting equation (13) can be obtained by integrating Eq. (12) or it can be directly drawn from Eq. (7) with the inclusion of a linear background term such as $B'_\pm|t|$ in the vicinity of T_{NA}. It is customary to include the first correction-to-scaling term [72] with the exponent 0.5 as we did in Eq. (13). Additionally, we notice here that in Eq. (13) we removed the constraint of the equality of the critical exponents below and above the transition. Also, at this stage we prefer using $\lambda = 1 - z$ instead of $\lambda = 1 - \alpha$. In principle, the transition temperature T_{NA} should be treated as a free parameter. It is well known that in fitting expressions such as Eq. (13) different parameters can be strongly correlated and to avoid this we reduced the free parameters in Eq. (13). At first we established the transition temperature T_{NA} with the fitting expression (12). In the preliminary fits T_{NA} was changed by iterations with steps of 0.002 K. The criteria for choosing the best value of T_{NA} were the minimum of the χ_ν^2 error function profile for the fits both below and above T_{NA} and the equality of the critical exponents $z = z'$. It is worth recalling that this procedure is quite similar to the one applied by Zywocinski and Wieczorek in the analysis of molar volume data [69]. The transition temperature value established by this method is $T_{NA} = 349.364$ K with the critical exponents $z = z' = 0.232 \pm 0.002$. Note that the above value of T_{NA} is 6 mK lower than the value obtained from the extrema of the $d(\Delta n)/dT$ vs T data and the one by polarizing microscopy. Since close to the transition point the contribution from the correction-to-scaling terms can be neglected, we set $D'_+ = D'_- = 0$. We then fitted our $\Delta n(T)$ data near the N-SmA transition to Eq. (13) with $T_{NA} = 349.364$ K fixed and the constraint $D'_+ = D'_- = 0$ using a nonlinear multiparameter fitting program discussed in the preceding section. The fitting results are presented in Table II. The values of the calculated critical exponents are stable to range shrinking and can be averaged to $z = 0.2417 \pm 0.0004$. The inclusion of the correction terms, i.e., $D'_+ \neq D'_- \neq 0$, did not improve the fit quality. Figure 9 presents the χ_ν^2 error function profile of simultaneous fits $\Delta n(T)$ above and below T_{NA} as a function of the critical exponent z. Additionally, as shown in Table II, $C'_+ \cong C'_- = \Delta n(T_{NA}) = 0.127\,35 \pm 0.000\,20$, thus we concluded that the N-SmA transition of $\overline{10}$.O.$\overline{4}$ is continuous together with the observation that there is no thermal hysteresis near T_{NA}.

As discussed above, the quotient $Q(T)$ has a regular background contribution that may result from the temperature dependence of Δn_{fit}; thus, for the fitting procedure we used the background quotient $Q_b(T)$ to eliminate this regular background. In the final step to determine the critical exponent z from the $\Delta n(T)$ data directly, we have subtracted the regular background $\Delta n_{\text{fit}}(T)$ from the birefringence data and then fitted the $\Delta n(T) - \Delta n_{\text{fit}}(T)$ data to the following fit expression:

$$\Delta n(T) - \Delta n_{\text{fit}}(T) = \begin{cases} A^+|t|^{1-z} + B^+|t| + C^+, & T > T_{NA} \\ A^-|t|^{1-z'} + B^-|t| + C^-, & T < T_{NA}. \end{cases} \tag{14}$$

Since the correction-to-scaling terms did not improve the fit quality appreciably during the previous fits, we did not include these correction terms in Eq. (14). While fitting the $\Delta n(T) - \Delta n_{\text{fit}}(T)$ data to Eq. (14) the N-SmA transition temperature was fixed at $T_{NA} = 349.364$ K, as was done previously. The fitting results are tabulated in Table II. The critical exponent values are insensitive to range shrinking and can be averaged to $z = 0.2305 \pm 0.0025$. Additionally, Fig. 10 depicts the χ_ν^2 error function profile of simultaneous fits $\Delta n(T) - \Delta n_{\text{fit}}(T)$ above and below T_{NA} as a function of the critical exponent z. The agreement is excellent with the exponent values obtained from separate fits. By taking into account the value of the critical exponent z obtained from various fitting expressions [Eqs. (12)–(14)] it can be seen that the critical exponent z extracted from the optical birefringence data and the α value from the calorimetric data are in good agreement. It should be noted here that the critical exponent z values are quite close to the α value when the regular background $\Delta n_{\text{fit}}(T)$ is subtracted during the fitting procedure [see the fitting expressions (12) and (14)]. Also note that the fits to Eq. (14) give better χ_ν^2 values than those to Eq. (13). Thus one can conclude that in order extract the critical exponent from the $\Delta n(T)$ data, the temperature dependence of $\Delta n_{\text{fit}}(T)$

TABLE II. Fitting parameters for the $\Delta n(T)$ data over the N-SmA transition region of $\overline{10}$.O.$\overline{4}$ [refer to Eqs. (13) and (14)]. Parameters in brackets were held constant at the quoted value. The N-SmA transition temperature $T_{NA} = 349.364$ K was held fixed in the fits. Here $|t|_{\max}$ denotes the upper limit of the fit and n is the number of data points in the fit.

Phase	z, z'	A'_+, A'_-	B'_+, B'_-	C'_+, C'_-	D'_+, D'_-	n	$\log_{10}\|t\|_{\max}$	χ_ν^2
N	0.2418	−0.6960	1.4642	0.1274	[0]	363	−2.67	1.85
	±0.0003	±0.0002	±0.010	±0.0001				
SmA	0.2417	0.7658	−1.6774	0.1273	[0]	738	−2.38	1.76
	±0.0001	±0.0009	±0.0038	±0.0001				
	z, z'	A^+, A^-	B^+, B^-	C^+, C^-		n	$\log_{10}\|t\|_{\max}$	χ_ν^2
N	0.230	−0.8188	2.481	0.0041		355	−2.67	1.03
	±0.003	±0.0002	±0.001	±0.0001				
SmA	0.231	0.8993	−2.666	0.0038		456	−2.58	1.14
	±0.002	±0.0002	±0.001	±0.0001				

should be taken into account during the fitting procedure. We emphasize that the value of the exponent z obtained by the rotating-analyzer method is more reliable than our previous results based on refractive index data [17]. From the obtained values of the exponent z ($=\alpha$) one can conclude that for the nonpolar smectogen (monolayer smectic-SmA_m) $\overline{10}$.O.$\overline{4}$ compound, the critical behavior of the N-SmA transition is dominated by crossover from 3D XY to tricriticality together with the observed McMillan ratio of $R_M = 0.972$. That is why the obtained z ($=\alpha$) values are significantly larger than the 3D XY for α.

As discussed in Sec. I, previously, the thermal conductivity anisotropy of 8CB and 9CB LCs was used by Marinelli and Mercuri [27] as a probe of the critical behavior of the nematic order parameter $S(T)$ close to the N-I and N-SmA transitions. Although the phenomenological model develop by the authors gives the same limiting behavior for the magnitude of the enhancement $\delta S = S - S_0$ near T_{NA}, instead of testing the theoretical relation $\lambda = 1 - \alpha$, the authors used $1 - \alpha$ directly for the critical behavior of the nematic order parameter $S(T)$ near T_{NA} to analyze their data [see Eqs. (8) and (9) in Ref. [27]]. They quoted α values directly from the literature. It is worth noticing that the fitting expression (14) used here is quite similar to the one used by Marinelli and Mercuri [see Eq. (9) in Ref. [27]] except for the background terms $B^{\pm}|t|$ and $C^{\pm}$. Nevertheless, in order to quantify their data the authors kept β fixed at the value of 0.37 for 8CB and 9CB LCs, which is inconsistent with the TCH for the N-I transition. Another issue is that the scaling condition $S(T = 0\text{ K}) = 1$ for the order parameter is not fulfilled in the data analysis given in Ref. [27], contrary to the one given in the present work. It should be emphasized that contrary to Marinelli and Mercuri, in the above analysis we prefer using $\lambda = 1 - z$ instead of $\lambda = 1 - \alpha$ and treat the exponent z as a free parameter. We have shown that there is excellent agreement between the z value extracted from optical data and the α value from calorimetric data. It should be remarked that the arguments and conclusions drawn here could be reached due to the high resolution (in both birefringence and temperature) of our measurements.

Furthermore, the temperature dependence of the order parameter $\langle|\Psi|^2\rangle$ can be achieved by means of the integrated x-ray-scattering intensity measurements [33]. Alternatively, the critical exponent λ in Eq. (7) can be extracted from from fitting the x-ray data to Eq. (7). These types of fittings were

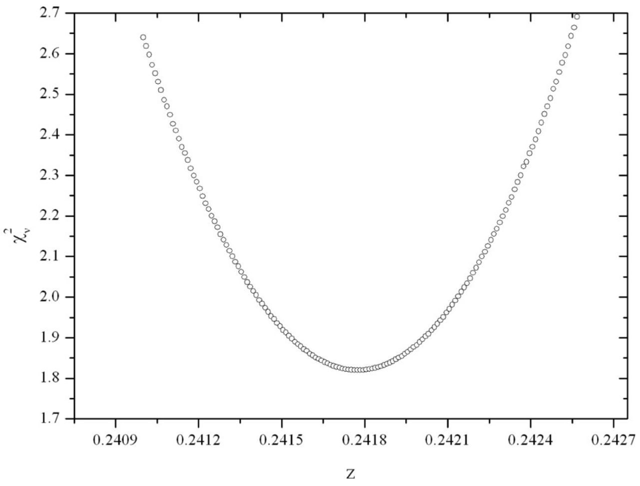

FIG. 9. The χ_ν^2 error function profile for fits of the $\Delta n(T)$ data deduced from stepwise variation of the critical exponent z. The fitting function is given by Eq. (13).

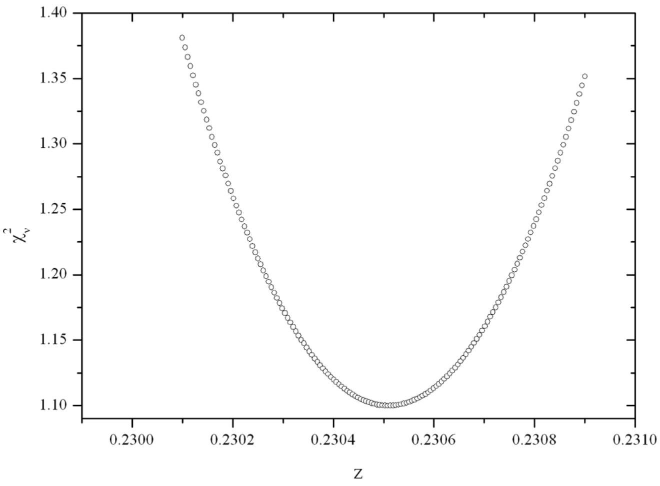

FIG. 10. Profile of the error function χ_ν^2 for the fits of the $\Delta n(T) - \Delta n_{\text{fit}}(T)$ data near T_{NA} obtained from stepwise variation of the critical exponent z by means of the fit function in Eq. (14).

performed by Chan *et al.* [33] for a series of LCs with a large variety of nematic ranges R_N ($=T_{NI} - T_{NA}$). For compounds with narrow R_N and close to the TCP ($\alpha_{\text{TCP}} = 0.5$), λ values close to $1 - \alpha$ were found. However, for compounds with wide R_N's, where one gets α values quite close to the 3D XY universality value $\alpha_{XY} = -0.007$, the authors observed that λ was not equal to $1 - \alpha$ and was much smaller than 1. The observed disagreement questioned the quantitative validity of the Landau–de Gennes free energy [33]. However, from our high-resolution $\Delta n(T)$ data for the $\overline{10}$.O.$\overline{4}$ LC exhibiting an effective α value between the 3D XY and tricritical values, we have concluded that $z = \alpha$ within the experimental uncertainty. Moreover, Beaubois *et al.* presented a comparative study of two LC compounds, namely, 8OCB and 4-octyloxybenzoyloxy-4′-cyanotolane C_8 tolane with different R_N based on the birefringence measurements [73]. The authors observed that for 8OCB exhibiting a narrow R_N there is a continuous transition-induced increase in the birefringence $n_e - n_o$ as soon as the fluctuations of the smectic-A order parameter Ψ in the nematic phase becomes sizable. On the contrary, for a C_8 tolane LC compound having a very large R_N from 99 °C to ≈247 °C, the authors observed that the $n_e - n_o$ vs T data are perfectly smooth and quite flat in the vicinity of T_{NA}. On the basis of their observations the authors concluded that the birefringence $n_e - n_o$ would not be sensitive to the coupling between the nematic and smectic-A order parameters for LCs exhibiting quite large R_N [73]. Sied *et al.* established the experimental two-component phase diagram for 8CB-8OCB by means of modulated differential scanning calorimetry to reveal the nature of the N-SmA transition [74]. The authors discussed that there exists a more or less common trend when the effective α exponents are plotted against the normalized nematic range R_N/T_{NI} ($=1 - R_M$). They concluded that 3D XY predictions take place for $R_N/T_{NI} \geqslant 0.04$ and when R_N becomes short ($R_N/T_{NI} \leqslant 0.04$) the crossover behavior to tricriticality is observed. It should be noted that the nCB and nOCB homologs and C_8 tolane LCs exhibit a SmA_d and monolayer SmA phase, namely, SmA_1, and the nonpolar $\overline{n}$.O.$\overline{m}$ homologs exhibit a SmA_m phase. Although the above conclusion that the crossover behavior to tricriticality is observed when $R_N/T_{NI} \leqslant 0.04$ seems valid for the $\overline{10}$.O.$\overline{4}$ LC with the observed numerical values of $R_N/T_{NI} = 0.028$ and $\alpha = 0.23$, a systematic calorimetric study on monolayer smectics (SmA_m) to determine whether such a trend between the effective α exponents and the normalized nematic range R_N/T_{NI} exists is lacking.

Based on the observations made by Beaubois *et al.* [73] and Sied *et al.* [74], it would be crucial to investigate whether there exists a relation between the normalized nematic range R_N/T_{NI} and the critical exponent z to reveal the agreement between the exponents z and α for a series of LC compounds having different R_N and especially different smectic-A phases such as SmA_d, SmA_1, and SmA_m since it is well known that the magnitude of the enhancement $\delta S = S - S_0$ of the nematic order parameter is smaller for SmA_d than for SmA_m LCs for a given R_M [12,31,49,71,75]. Additionally, these systematic optical birefringence measurements are essential on LCs having different R_N in order to understand the sensitivity of the optical birefringence on the N-SmA coupling. The above-mentioned issues are not clear at the moment and deserve to be investigated systematically based on high-resolution (in both temperature and birefringence) optical birefringence experiments.

V. CONCLUSION

In this work we have presented high-resolution (in both the birefringence and temperature) experimental data for the temperature dependence of the optical birefringence for the liquid crystal 4-butyloxyphenyl-4′-decyloxybenzoate ($\overline{10}$.O.$\overline{4}$). The birefringence data cover nematic and smectic-A phases of the $\overline{10}$.O.$\overline{4}$ LC compound. The measurements are based on a rotating-analyzer method, which is known to be a very accurate interference method. It is worthwhile noting that this high-resolution experimental study is for the temperature dependence of optical birefringence of $\overline{n}$.O.$\overline{m}$ nonpolar monolayer smectogens. We have discussed the critical behavior of the nematic order parameter at the N-I transition in detail by comparing our results with the latest reports found in the literature. By using the Vuks-Chandrasekhar-Madhusudana model for the internal electric field we have obtained the temperature behavior of the nematic order parameter $S(T)$. From the data sufficiently far away from the smectic-A phase we have extracted the critical exponent β describing the limiting behavior of $S(T)$ near the N-I transition. The average value of the critical exponent β was found to be $\langle\beta\rangle = 0.2507 \pm 0.0010$. The critical exponent value is in agreement with the value given by the tricritical hypothesis with $\beta = 0.25$ and excludes higher theoretical values. Additionally, we have concluded that by comparing our results with the reported results in the literature [16,17,19,20,22], the isotropic internal field assumption by the VCM model and the approximation used while deriving Eq. (4) are adequate to extract the critical behavior of the order parameter $S(T)$ from the optical birefringence data.

Furthermore, we have also shown that the so-called effective birefringence $\Delta n^* \propto n(T)[n_e(T) + n_o(T)]/2$ used by Kityk *et al.* [12,13] and the quantity $\Delta n^{**} \propto \Delta n(T) n_I$ are deficient to represent the temperature behavior of $S(T)$, contrary to the claim by Kityk *et al.* Recently, Simoes *et al.* [62,63] investigated the behavior of the nematic order parameter in the entire nematic range for the LC samples exhibiting only an isotropic liquid, nematic, and crystalline phase sequence by rescaling the experimental data obtained from refractive index, anisotropy in magnetic susceptibility, dielectric constant, and thermal conductivity measurements. They concluded that along the entire N range $\beta = 0.25$, which is the value given by the TCH. Although it is established that experimental data on the N-I transition can be well described by the TCH, the characteristic temperatures (T_{NI}, T^*, and T^{**}) and their relative differences seem to depend on the experimental method and still remain a puzzle [56–58]. By comparing our results, namely, the $T^{**} - T_{NI}$ difference, with the reported values obtained from various experimental data, we concluded that the optical measurements seem to be more appropriate to get reliable values for the spinodal temperature T^{**}. Finally, we emphasize that the data used by Simoes *et al.* belong to LC compounds having only a nematic phase without any other liquid crystalline phase. In contrast, LCs compounds such as 8CB [16] and $\overline{10}$.O.$\overline{4}$ exhibit pretransitional smectic behavior that continues up to 4 K above the N-SmA

transition. It would be intriguing to investigate whether the similar homogenous global behavior of the nematic order parameter $S(T)$ would be seen for LC compounds exhibiting pretransitional smectic behavior and whether there would be a universal pretransitional temperature range above T_{NA}. A theory comprising not only the global behavior of the order parameter $S(T)$ observed by Simoes *et al.* but also the pretransitional smectic behavior above T_{NA} is lacking and the latter subject deserves further investigation both theoretically and experimentally.

No discontinuous behavior in the optical birefringence at the N-SmA transition was detected. Thus we concluded that the N-SmA transition of the $\overline{10}$.O.$\overline{4}$ LC is continuous. We have presented a detailed analysis of the critical behavior of the nematic order parameter $S(T)$ in the vicinity of the N-SmA transition in Sec. IV B . In a temperature range of about 4 K above and below the N-SmA transition, pretransitional evidence for the N-SmA coupling has been observed. From the analysis of the optical birefringence data above and below the N-SmA transition temperature by means of various fitting expressions [Eqs. (12)–(14)], it has been found that the temperature derivative of the nematic order parameter $S(T)$ near T_{NA} exhibits a power-law divergence with a critical exponent z. The critical exponent value is quite insensitive to range shrinking and can be averaged to $z = 0.2303 \pm 0.0035$. It should be noted that, within experimental uncertainty, the obtained experimental value of the exponent z is the same as the value of the exponent α ($\alpha = 0.23 \pm 0.01$) from adiabatic scanning calorimetry for the specific heat capacity [46]. Excellent agreement between the critical exponent z extracted from optical birefringence data and the α value from calorimetric data is clearly established. It should be noted once again that owing to the high sensitivity and temperature resolution of our optical birefringence measurements, we could reach the conclusions presented in this work. Thus one can conclude that the rotating-analyzer method can be successfully applied to study the pretransitional effects in the vicinity of the N-SmA transition in LCs. The method has proven to be a very accurate and easy way to reveal the order of the N-SmA transition as compared to calorimetric methods.

A systematic investigation of whether there is agreement between the exponents z and α for other LC compounds is lacking. As discussed in Sec. IV B, the relation between the exponents z and α or the validity of the scaling relation $\lambda = 1 - \alpha$ deserve to be investigated systematically to reveal the sensitivity of the optical birefringence on the N-SmA coupling for a series of LC compounds having different R_N and especially different smectic-A phases such as SmA_d, SmA_1, and SmA_m. The analysis of the birefringence data near the N-SmA transition particularly for LC compounds exhibiting a partially bilayer SmA phase, namely, SmA_d, is beyond the scope of the present paper.

ACKNOWLEDGMENT

This work was supported by the Research Fund of Istanbul Technical University under Grants No. 34412, No. 34254, and No. 34824.

---

[1] P. G. de Gennes and J. Prost, *The Physics of Liqiud Crystals*, 2nd ed. (Oxford University Press, New York, 1993).

[2] S. Kumar, *Liquid Crystals* (Cambridge University Press, Cambridge, 2001).

[3] P. J. Collings and M. Hird, *Introduction to Liquid Crystals: Chemistry and Physics* (Taylor & Francis, London, 1997).

[4] G. Pelzl, in *Handbook of Liquid Crystals*, edited by D. Demus, J. Goodby, G. W. Gray, H. W. Spiess, and V. Vill (Wiley-VCH, Weinheim, 1998), Vol. 2A, p. 128, and references cited therein.

[5] H. Hirschmann and V. Reiffenrath, in *Handbook of Liquid Crystals* (Ref. [4]), p. 199.

[6] S. Urban *et al.*, Phys. Chem. Chem. Phys. **5**, 924 (2003).

[7] W. Kuczynski, B. Zywucki, and J. Malecki, Mol. Cryst. Liq. Cryst. **381**, 1 (2002), and references cited therein; M. Ramakrishna *et al.*, *ibid.* **528**, 49 (2010).

[8] B. Kundu, R. Pratibha, and N. V. Madhusudana, Phys. Rev. Lett. **99**, 247802 (2007); R. Pratibha, N. V. Madhusudana, and B. K. Sadashiva, Phys. Rev. E **71**, 011701 (2005); S. Dhara and N. V. Madhusudana, Phase Transit. **81**, 561 (2008).

[9] T. Moses and J. Reeves, Liq. Cryst. **35**, 1395 (2008).

[10] Y. Yusuf, Y. Sumisaki, and S. Kai, Chem. Phys. Lett. **382**, 198 (2003).

[11] F. Beaubois and J. P. Marcerou, Europhys. Lett. **36**, 111 (1996).

[12] G. Chahine *et al.*, Phys. Rev. E **82**, 011706 (2010); A. V. Kityk and P. Huber, Appl. Phys. Lett. **97**, 153124 (2010).

[13] A. V. Kityk, K. Knorr, and P. Huber, Phys. Rev. B **80**, 035421 (2009); A. V. Kityk *et al.*, Phys. Rev. Lett. **101**, 187801 (2008).

[14] The abbreviations in nCB and nOCB refer to homologous 4-alkyl-4′-cyanobiphenyl and 4-alkyloxy-4′-cyanobiphenyl liquid crystalline compounds, respectively. Here n refers to the number of carbon atoms in the alkyl chain for the former and the alkyloxy chain for the latter.

[15] A. J. Leadbetter, R. M. Richardson, and C. N. Colling, J. Phys. (Paris) Colloq. **36**, C1-37 (1975).

[16] I. Chirtoc, M. Chirtoc, C. Glorieux, and J. Thoen, Liq. Cryst. **31**, 229 (2004).

[17] S. Yildiz, H. Özbek, C. Glorieux, and J. Thoen, Liq. Cryst. **34**, 611 (2007).

[18] M. S. Zakerhamidi *et al.*, J. Mol. Liq. **157**, 119 (2010); A. Prasad and M. K. Das, Phase Transit. **83**, 1072 (2010); J. Li, S. Gauza, and S. T. Wu, J. Appl. Phys. **96**, 19 (2004); P. Sathyanarayana *et al.*, Phys. Rev. E **82**, 050701 (2010).

[19] S. S. Sastry, T. V. Kumari, S. S. Begum, and V. V. Rao, Liq. Cryst. **38**, 277 (2011); S. S. Sastry, T. V. Kumari, K. Mallika, B. G. S. Rao, S.-T. Ha, and S. Lakshminarayana, *ibid.* **39**, 295 (2012); J. L. Kumari, P. V. D. Prasad, D. M. Latha, and V. G. K. M. Pisipati, Phase Transit. **85**, 52 (2012).

[20] M. Ramakrishna *et al.*, Mol. Cryst. Liq. Cryst. **528**, 49 (2010); V. G. K. M. Pisipati and P. V. D. Prasad, *ibid.* **506**, 13 (2009); P. V. D. Prasad and V. G. K. M. Pisipati, *ibid.* **511**, 102 (2009).

[21] S. Chakraborty and A. Mukhopadhyay, Phase Transit. **79**, 201 (2006); **82**, 115 (2009); S. D. Sarkar and B. Choudhury, *ibid.* **85**, 85 (2012).

[22] I. Haller, Prog. Solid State Chem. **10**, 103 (1975).

[23] J. Thoen, in *Physical Properties of Liquid Crystals*, edited by D. Demus, J. Goodby, G. W. Gray, H. W. Spiess, and V. Vill (Wiley-VCH, Weinheim, 1999).

[24] M. Marinelli, F. Mercuri, and U. Zammit, in *Heat Capacities: Liquids, Solutions, and Vapours*, edited by E. Wilhelm and T. M. Letcher (Royal Society of Chemistry, London, 2010).

[25] J. Thoen and T. Bose, in *Handbook of Low and High Dielectric Constant Materials and Their Applications*, edited by H. S. Nalwa, Vol. 1 (Academic, London, 1999).

[26] J. Thoen and G. Menu, Mol. Cryst. Liq. Cryst. **97**, 163 (1983).

[27] M. Marinelli and F. Mercuri, Phys. Rev. E **61**, 1616 (2000).

[28] C. W. Garland, in *Liquid Crystals*, edited by S. Kumar (Cambridge University Press, Cambridge, 2001).

[29] J. Thoen, Int. J. Mod. Phys. B **9**, 2157 (1995).

[30] P. D. Roy, A. Prasad, and M. K. Das, J. Phys.: Condens. Matter **21**, 075106 (2009); A. Prasad and M. K. Das, *ibid.* **22**, 195106 (2010).

[31] K. C. Lim and J. T. Ho, Phys. Rev. Lett. **40**, 944 (1978).

[32] E. F. Gramsbergen and W. H. de Jeu, J. Chem. Soc. Faraday Trans. 2 **84**, 1015 (1988).

[33] K. K. Chan, M. Deutsch, B. M. Ocko, P. S. Pershan, and L. B. Sorensen, Phys. Rev. Lett. **54**, 920 (1985).

[34] M. E. Fisher and A. Aherony, Phys. Rev. Lett. **31**, 1238 (1973).

[35] The abbreviation $\overline{n}$.O.$\overline{m}$ refers to homologous 4-alkyloxyphenyl esters of 4-alkyloxybenzoic acid or, alternatively, 4-alkyloxyphenyl-4′-alkyloxybenzoate.

[36] C. W. Garland and G. Nounesis, Phys. Rev. E **49**, 2964 (1994).

[37] M. A. Anisimov, P. E. Cladis, E. E. Gorodetskii, D. A. Huse, V. E. Podneks, V. G. Taratuta, W. van Saarloos, and V. P. Voronov, Phys. Rev. A **41**, 6749 (1990).

[38] M. A. Anisimov, Mol. Cryst. Liq. Cryst. **162A**, 1 (1988).

[39] E. N. Keller, E. Nachaliel, D. Davidov, and C. Böffel, Phys. Rev. A **34**, 4363 (1986).

[40] T. Chan, Ch. Bahr, G. Heppke, and C. W. Garland, Liq. Cryst. **13**, 667 (1993).

[41] T. Brauniger and B. M. Fung, J. Chem. Phys. **102**, 7714 (1995).

[42] Ch. Bahr and G. Heppke, Phys. Rev. Lett. **65**, 3297 (1990); Phys. Rev. A **41**, 4335 (1990).

[43] S. Yildiz and A. Nesrullajev, Physica A **385**, 25 (2007).

[44] H. Özbek, S. Yildiz, Ö. Pekcan, and A. N. Berker, Phase Transit. **75**, 301 (2002); Int. J. Mod. Phys. B **15**, 2161 (2001).

[45] S. Yildiz, E. O. Zayim, Ö. Pekcan, and H. Özbek, Int. J. Mod. Phys. B **24**, 4305 (2010).

[46] K. Denolf, B. Van Roie, C. Glorieux, S. Yildiz, H. Özbek, and J. Thoen, Mol. Cryst. Liq. Cryst. **477**, 497 (2007).

[47] M. D. Gupta, A. Mukhopadhyay, and K. Czuprynski, Phase Transit. **83**, 284 (2010).

[48] D. A. Dunmur, in *Physical Properties of Liquid Crystals: Nematics*, edited by D. A. Dunmur, A. Fukuda, and G. R. Luckhurst (The Institution of Electrical Engineers, London, 2002).

[49] K. C. Lim and J. T. Ho, Mol. Cryst. Liq. Cryst. **47**, 173 (1978).

[50] V. Tsvetkov, Acta Physicochim. (USSR) **16**, 132 (1942).

[51] M. Vuks, Opt. Spectrosc. **20**, 361 (1966); S. Chandrasekhar and N. V. Madhsudana, J. Phys. (Paris) Colloq. **30**, C4-24 (1969).

[52] H. E. J. Neugebauer, Can. J. Phys. **32**, 1 (1954); A. Saupe and W. Maier, Z. Naturforsch. Teil A **16**, 816 (1961); H. S. Subramhanyam and D. Krishnamurthi, Mol. Cryst. Liq. Cryst. **22**, 239 (1973).

[53] S. Singh, Phys. Rep. **324**, 107 (2000).

[54] P. G. de Gennes, Mol. Cryst. Liq. Cryst. **21**, 49 (1973).

[55] P. R. Bevington and D. K. Robinson, *Data Reduction and Error Analysis for The Physical Sciences*, 3rd ed. (Mc Graw Hill, New York, 2003).

[56] P. Cusmin *et al.*, J. Phys. Chem. B **111**, 8974 (2007).

[57] S. J. Rzoska, J. Ziolo, W. Sulkowski, J. Jadzyn, and G. Czechowski, Phys. Rev. E **64**, 052701 (2001).

[58] A. Zywocinski, J. Phys. Chem. B **107**, 9491 (2003).

[59] P. H. Keyes, Phys. Lett. A **67**, 132 (1978).

[60] M. A. Anisimov, S. R. Garber, V. S. Esipov, V. M. Mamnitskii, G. I. Ovodov, L. A. Smolenko, and E. L. Sorkin, JETP **45**, 1042 (1977).

[61] M. A. Anisimov, *Critical Phenomena in Liqiuds and Liquid Crystals* (Gordon and Breach, Philadelphia, 1990).

[62] M. Simoes and D. S. Simeao, Phys. Rev. E **74**, 051701 (2006), and references cited therein.

[63] M. Simoes, D. S. Simeao, and K. E. Yamaguti, Liq. Cryst. **38**, 935 (2011), and references cited therein.

[64] W. H. de Jeu, *Physical Properties of Liquid Crystalline Materials* (Gordon and Breach, New York, 1980).

[65] S. J. Picken, L. Noirez, and G. R. Luckhurst, J. Chem. Phys. **109**, 7612 (1998).

[66] A. Buka and W. H. de Jeu, J. Phys. (Paris) **43**, 361 (1982).

[67] J. Thoen, in *Heat Capacities: Liquids, Solutions, and Vapours*, edited by E. Wilhelm and T. M. Letcher (Royal Society of Chemistry, London, 2010).

[68] G. Cordoyiannis, Chandra Shekhar Pati Tripathi, C. Glorieux, and J. Thoen, Phys. Rev. E **82**, 031707 (2010); J. Thoen, G. Cordoyiannis, and C. Glorieux, Liq. Cryst. **36**, 669 (2009).

[69] A. Zywocinski and S. A. Wieczorek, J. Phys. Chem. B **101**, 6970 (1997).

[70] A. Zywocinski, S. A. Wieczorek, and J. Stecki, Phys. Rev. A **36**, 1901 (1987).

[71] E. Anesta, G. S. Iannacchione, and C. W. Garland, Phys. Rev. E **70**, 041703 (2004), and references cited therein.

[72] C. Bagnuls and C. Bervillier, Phys. Rev. B **32**, 7209 (1985).

[73] F. Beaubois, T. Claverie, J. P. Marcerou, J. C. Rouillon, H. T. Nguyen, C. W. Garland, and H. Haga, Phys. Rev. E **56**, 5566 (1997).

[74] M. B. Sied, D. O. Lopez,, J. L. Tamarit, and M. Barrio, Liq. Cryst. **29**, 57 (2002).

[75] S. Erkan, Ph.D. thesis, Istanbul Technical University, 2012.